Emodin inhibits TGF-β2 by activating the FOXD3/miR-199a axis in ovarian cancer cells *in vitro*

KEJUAN SONG*, TENG LV*, YULONG CHEN, YUCHAO DIAO, QIN YAO and YANKUI WANG

Department of Obstetrics and Gynecology, The Affiliated Hospital of Qingdao University, Qingdao, Shandong 266003, P.R. China

Received August 10, 2017; Accepted March 2, 2018

DOI: 10.3892/or.2018.6301

Abstract. Ovarian cancer is a highly metastatic malignancy and a leading cause of cancer-related death in postmenopausal women. Emodin is a natural anthraquinone isolated from several traditional Chinese medicines including Rhubarb and *Polygonum cuspidatum*. Recently, emodin was demonstrated to reduce the growth of human ovarian carcinoma cells. However, the mechanism remains unclear. In the present study, we identified that transforming growth factor (TGF)-β2 was significantly affected by emodin treatment in A2780 cells using microarray analysis. MicroRNA (miR)-199a was predicted as a potential miRNA targeting TGF-β2 by *in silico* prediction using TargetScan. The mRNA and protein levels of TGF-β2 were both significantly reduced by miR-199a. Spearman's correlation analysis revealed a significant correlation between the expression level of miR-199a and TGF-β2 in human ovarian cancer specimens. Silencing of miR-199a with miR-199a inhibitor significantly restored the reduction in TGF-β2 expression induced by emodin. Additionally, cell viability and colony formation of A2780 cells were markedly inhibited by emodin treatment, which was mediated by miR-199a. We analyzed the primary mature miR-199a-1 and miR-199a-2 transcripts in A2780 cells treated with emodin or dimethyl sulfoxide (DMSO) and found that only pri-miR-199a-1 was regulated by emodin. A conserved binding site of Forkhead box D3 (FOXD3) was identified within pri-miR-199a-1. We further revealed that miR-199a expression was significantly regulated by FOXD3. Taken together, the present study demonstrated that emodin may directly promote FOXD3 expression and sequentially activates miR-199a, which in turn suppresses the expression of TGF-β2 to reduce cell viability and colony formation of A2780 cells.

Correspondence to: Dr Qin Yao or Dr Yankui Wang, Department of Obstetrics and Gynecology, The Affiliated Hospital of Qingdao University, 1677 Wutaishan Road, Qingdao, Shandong 266003, P.R. China
E-mail: dr_yaoqin@126.com
E-mail: qdwykpro@163.com

*Contributed equally

Key words: ovarian cancer, TGF-β2, miR-199a, FOXD3

Introduction

Ovarian cancer is a highly metastatic malignancy. The survival rate of ovarian cancer remains low and has only slightly increased during the last several decades, as many patients are still diagnosed at an advanced stage. In the United States, ovarian cancer is the fifth leading cause of cancer-related death in postmenopausal women (1). Recently, the mortality rate of ovarian cancer patients demonstrated an increasing trend in China from 2000 to 2011 (2). The main reason for this high mortality rate is not only the fact that many patients are diagnosed at an advanced stage, but also the development of drug-resistance such as cisplatin-resistance despite improvements in chemotherapies. Therefore, in addition to the discovery of novel targets for early detection, new therapeutic strategies are necessary to improve the outcomes of patients with ovarian cancer.

Emodin is a natural anthraquinone isolated from several plants including Rhubarb and *Polygonum cuspidatum* that are widely applied in traditional Chinese medicine (3). It has been demonstrated that emodin exhibits an antitumor effect *in vitro* through several mechanisms. Inhibition of angiogenesis by suppressing angiogenesis-associated microRNA (miR)-155, miR-210 and miR-20b was observed in pancreatic cancer (4). Gastric cancer cell proliferation was suppressed by emodin via downregulation of c-myc expression (5). Additionally, studies have revealed that emodin induces cell cycle arrest and apoptosis in colon cancer cells by increasing the expression of caspase-6 (6) and p53 (7). Recent studies have demonstrated that emodin also plays an inhibitory role in transforming growth factor (TGF)-β-induced epithelial-mesenchymal transition (EMT) (8,9). A low concentration of emodin was shown to enhance paclitaxel-induced apoptosis (10). Combined use of emodin and cisplatin reduced the growth of human ovarian carcinoma cells by downregulating multidrug resistance-related protein 1 expression (11).

Although studies have investigated the mechanisms underlying the effects of emodin on ovarian cancer since the last decade, the conclusions are inconsistent. A deeper insight into the *in vitro* role of emodin in inhibiting ovarian cancer cell growth is warranted. In the present study, we demonstrated

that emodin inhibited the expression of TGF-β2 by regulating miR-199a and forkhead box D3 (FOXD3) in ovarian cancer cells.

Materials and methods

Cell culture. A2780 human epithelial ovarian cancer cell line was purchased from the Cell Bank of the China Academy of Sciences (Shanghai, China). Cells were cultured in RPMI-1640 medium modified (HyClone Laboratories; GE Healthcare, Chicago, IL, USA), supplemented with 10% fetal bovine serum (FBS), 100 U/ml penicillin and 100 μg/ml streptomycin in humidified air at 37˚C with 5% CO_2. For treatment, 20 μM emodin (cat. no. 30269, purity ≥97.0%; Sigma-Aldrich; Merck KGaA, Darmstadt, Germany) or dimethyl sulfoxide (DMSO) was added to the cell medium for 0, 6, 12 or 24 h. Trypsin (0.25%) was used to detach the cells from the plates.

RNA extraction and cDNA synthesis. Total RNA was extracted using TRIzol reagent (Invitrogen; Thermo Fisher Scientific, Inc., Waltham, MA, USA) following the manufacturer's protocol. RNA purity was assessed by Thermo NanoDrop 2000 (Thermo Fisher Scientific, Inc.) by standard absorbance ratios as A260/A280 ≥1.8 and A260/A230 ≥1.5. Complementary DNAs were synthesized from 1 μg of total RNA using TaqMan Reverse Transcription reagents (Life Technologies; Thermo Fisher Scientific, Inc.).

Microarray analysis. A2780 cells were pre-treated with 20 μM emodin or DMSO for 24 h. To quantify miRNAs, TaqMan® MicroRNA Reverse Transcription kit (Invitrogen; Thermo Fisher Scientific, Inc.) was used. For the microarray assay, RNA was amplified with the GeneChip 3'IVT Express kit (Affymetrix Inc.; Thermo Fisher Scientific, Inc.). Quality of the samples was verified by the NanoDrop results. The amplified transcripts were hybridized to Affymetrix Human Genome U133 Plus 2.0 Array (Affymetrix; Thermo Fisher Scientific, Inc.) according to the manufacturer's protocol. The results were analyzed using GeneSpring 12.6 (Agilent Technologies, Inc., Santa Clara, CA, USA).

Computational miRNA target prediction and quantitative real-time PCR. TargetScan 6.0 (http://www.targetscan.org/) was used to predict potential miRNAs binding to TGF-β2. The predicted miRNAs were tested using quantitative real-time (qRT)-PCR. For miRNA analysis, qRT-PCR was performed using TaqMan microRNA Assay (Applied Biosystems; Thermo Fisher Scientific, Inc.) according to the manufacturer's instructions with specific TaqMan probes (Applied Biosystems; Thermo Fisher Scientific, Inc.). For quantitation of mRNA, a Bio-Rad CFX96 Real-Time PCR system (Bio-Rad Laboratories, Hercules, CA, USA) was employed according to the manufacturer's instructions. All mRNA and miRNA quantification data were normalized to GAPDH and U6, respectively. hTGF-β2 sense, 5'-TGGTGAAAGCAGAGTTCAGAG-3' and antisense, 5'-CACAACTTTGCTGTCGATGTAG-3'; GAPDH sense, 5'-AGCCTCCCGCTTCGCTCTCT-3' and antisense, 5'-GCGCCCAATACGACCAAATCCGT-3'; U6 sense, 5'-GCTTCGGCAGCACATATACTAAAAT-3' and antisense, 5'-CGCTTCACGAATTTGCGTGTCAT-3'; FOXD3 sense, 5'-GTCCGCTGGGAATAACTTTCCGTA-3' and antisense, 5'-ATGTACAAAGAATGTCCCTCCCACCC-3' were used

Luciferase assay. The three mutations in the TGF-β2 3' untranslated region (UTR) and pGL3-Report pri-miR-199a-1 constructs were generated using QuikChange Site-Directed Mutagenesis kits (Agilent Technologies, Inc., Santa Clara, CA, USA). Cells were transfected using Lipofectamine 2000 (Invitrogen; Thermo Fisher Scientific, Inc.). Cells ($5x10^3$) were plated into 96-well plates and incubated overnight before transfection. Luciferase activities were measured by a Dual-Luciferase reporter assay system (Promega, Madison, WI, USA) according to the manufacturer's instructions. *Renilla* luciferase vector (Promega) was applied as an internal control.

Western blotting. Protein extract was obtained using RIPA Lysis Buffer (Beyotime Institute of Biotechnology, Haimen, China) containing 1% phenylmethylsulfonyl fluoride (PMSF; Sigma-Aldrich; Merck KGaA). Equal amounts of samples were loaded and separated by 10% SDS-PAGE and transferred onto a nitrocellulose (NC) membrane (Sigma-Aldrich; Merck KGaA). Membranes were blocked with 5% skim milk and then incubated with anti-TGF-β2 produced in rabbit (1:400; cat. no. SAB4502956; Sigma-Aldrich; Merck KGaA) and GAPDH produced in rabbit (1:200; cat. no. G9546; Sigma-Aldrich; Merck KGaA) diluted in Tris-buffered saline containing 0.1% (v/v) Tween-20 (PBST) overnight at 4˚C. After washing with PBST, the membranes were incubated with horseradish peroxidase-conjugated goat anti-rabbit or anti-mouse IgG (cat. no. 65-6120; Thermo Fisher Scientific, Inc.). The results were visualized by ECL kit (Thermo Fisher Scientific, Inc.) and exposed to X-ray film (Thermo Fisher Scientific, Inc.).

Cell viability. Cell viability was measured by Cell Counting Kit-8 (CCK-8) assay purchased from BestBio (Shanghai, China). Briefly, cells were seeded at a density of 3,500 cells/well in a 96-well plate. Emodin (20 μM) was added into each well after an overnight incubation. After 48 h of transfection, 10 μl of diluted CCK-8 solution was added to each well and incubated for 2 h at 37˚C. The absorbance values were read at wavelengths of 450 nm using a microplate reader (Bio-Rad Laboratories).

Colony formation. For the colony formation assay, ovarian cancer cells were pre-treated with 20 μM emodin for 24 h. Then, the cells were seeded in 6-well plates at a density of 300 cells/well. After 2 weeks of incubation, the cells were washed twice with phosphate-buffered saline (PBS) and fixed in 4% paraformaldehyde-methanol for 10 min. The colonies were stained using 0.1% crystal violet (Sigma-Aldrich; Merck KGaA) and the number of colonies were counted. The colonies were calculated as the mean number of cells in 10 randomly selected fields using phase-contrast microscopy (Olympus Corp., Tokyo, Japan)

Human ovarian cancer specimens. Human ovarian cancer specimens were derived from the patients in our hospital between May 2016 and March 2017. Written consent has

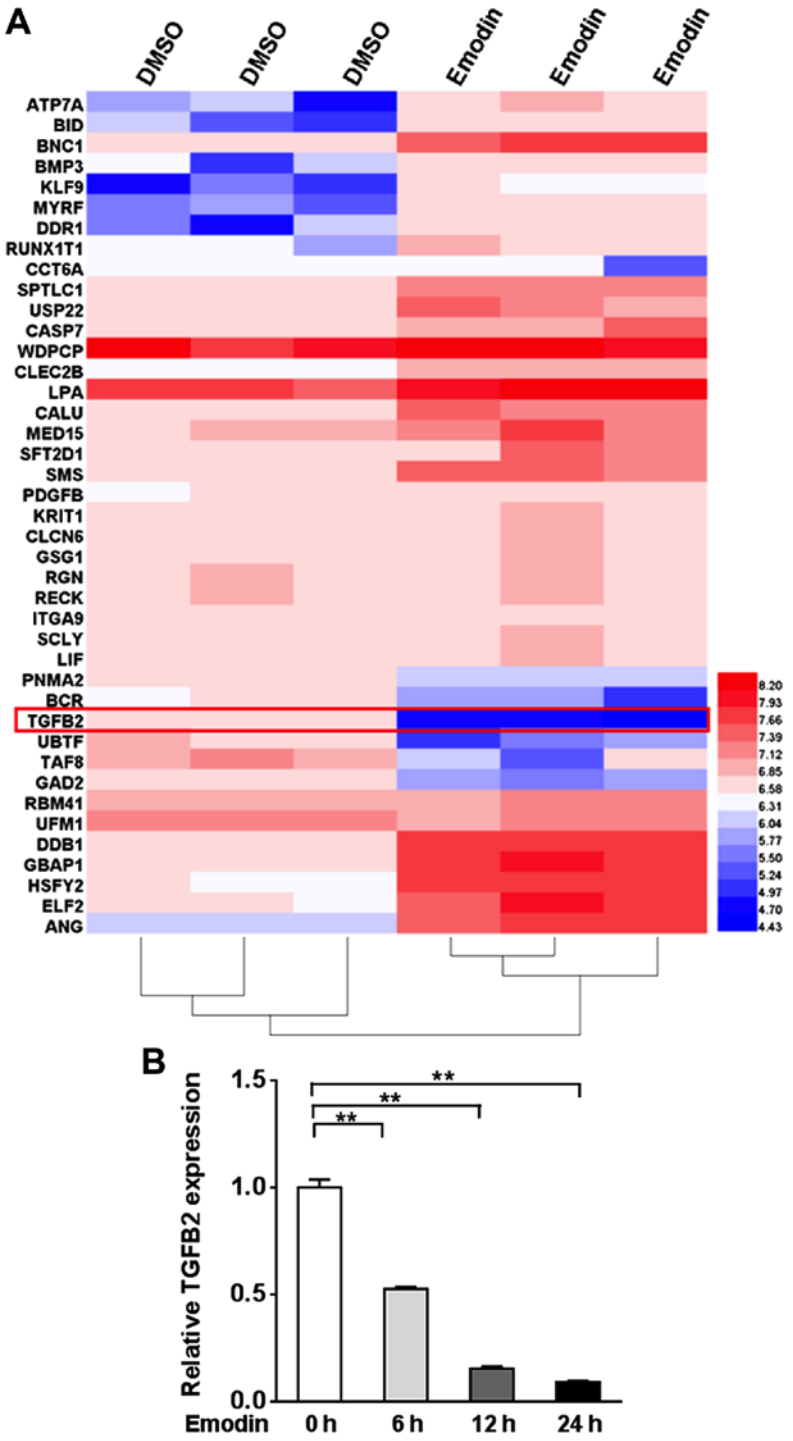

Figure 1. Emodin induces the downregulation of TGF-β2 in ovarian cancer. (A) A2780 cells were treated with 20 μM emodin or DMSO for 24 h. Microarray was employed to analyze the gene expression profiles. (B) A2780 cells were treated with 20 μM emodin or DMSO for 0, 6, 12 or 24 h. The TGF-β2 expression level was measured by qRT-PCR. Data are presented as mean ± SD from three independent experiments with triple replicates per experiment. **P<0.01.

been obtained from each participant. The present study was approved by the ethics committee in our hospital.

Statistical analysis. All data are shown as the mean ± SD from three independent experiments. Two-tailed Student's t-test was used to analyze the differences between samples. Spearman's correlation coefficient was employed for analysis of the correlation between the expression levels of miR-199a and TGF-β2 in human ovarian cancer specimens. Statistical significance was considered as P<0.05.

Results

Downregulation of TGF-β2 by emodin in A2780 cells. To assess the genes affected by emodin, we performed microarray analysis in A2780 cells treated with emodin compared to cells treated with DMSO. Among all of the gene transcripts, TGF-β2 was markedly reduced ~1.5-fold in the emodin-treated A2780 cells (Fig. 1A). We further examined the TGF-β2 expression level by qRT-PCR in A2780 cells treated with emodin for 0, 6, 12 and 24 h. TGF-β2 expression was significantly lower than

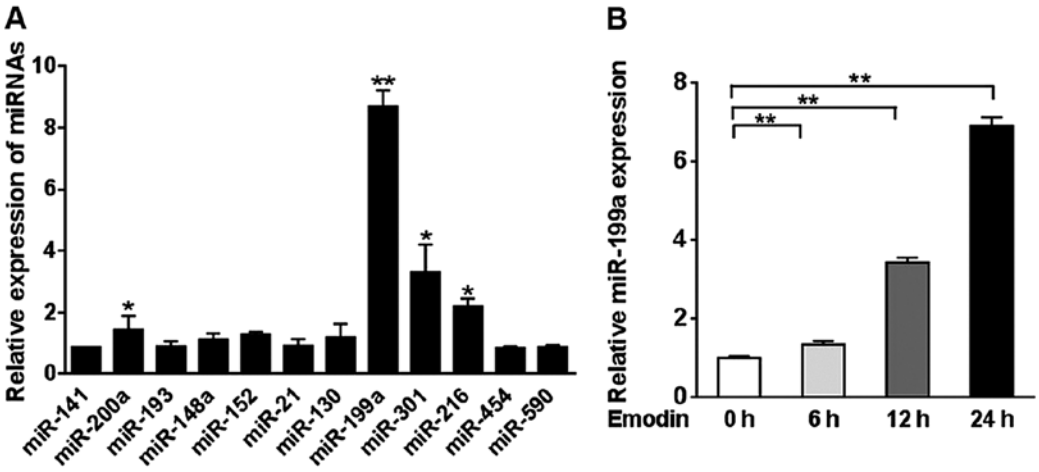

Figure 2. miR-199a expression is elevated by emodin. (A) The expression levels of 12 miRNAs were analyzed by qRT-PCR in A2780 cells treated with 20 μM emodin or DMSO. The values from emodin-treated cells were normalized to DMSO control and U6 levels were used as internal control. (B) A2780 cells were treated with 20 μM emodin or DMSO for 0, 6, 12 or 24 h. miR-199a expression levels were analyzed by qRT-PCR. Data are presented as the means ± SD from three independent experiments with triple replicates per experiment. *P<0.05, **P<0.01, indicate significant difference compared to the DMSO group or 0 h of emodin treatment.

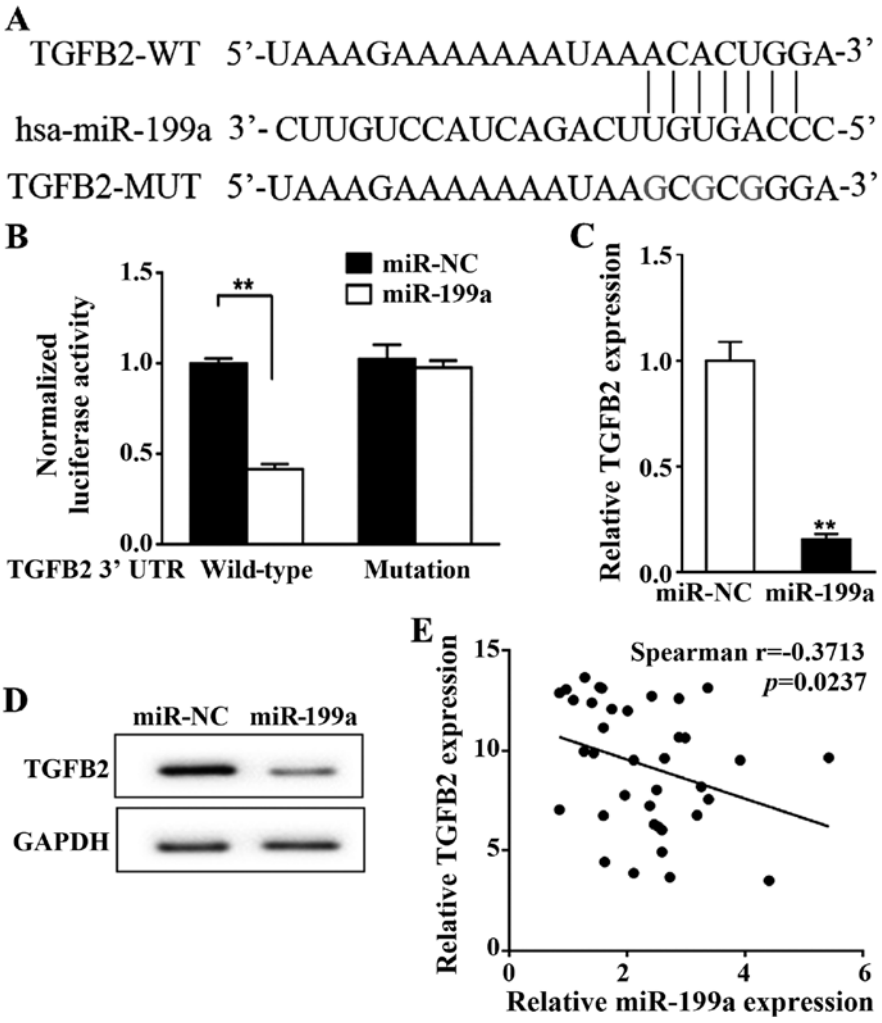

Figure 3. miR-199a directly regulates TGF-β2. (A) Putative seed-matching sites or mutant sites (red) in miR-199a 3'-UTR of TGF-β2. (B) Luciferase reporter assay was performed on A2780 cells to detect the relative transcriptional activities of wild-type and mutated TGF-β2 reporters. (C and D) A2780 cells were transfected with miR-199a or control miR-NC mimics. After 48 h, the expression levels of TGF-β2 were analyzed by qRT-PCR and western blotting. Data are presented as the means ± SD from three independent experiments with triple replicates per experiment. **P<0.01, indicates a significant difference compared to the miR-NC group. (E) The expression levels of miR-199a and TGF-β2 in human ovarian cancer specimens (n=37) was determined by qRT-PCR analysis. Spearman's correlation analysis was used to determine the correlation between miR-199a and TGF-β2 in human ovarian cancer specimens (n=37). UTR, untranslated region.

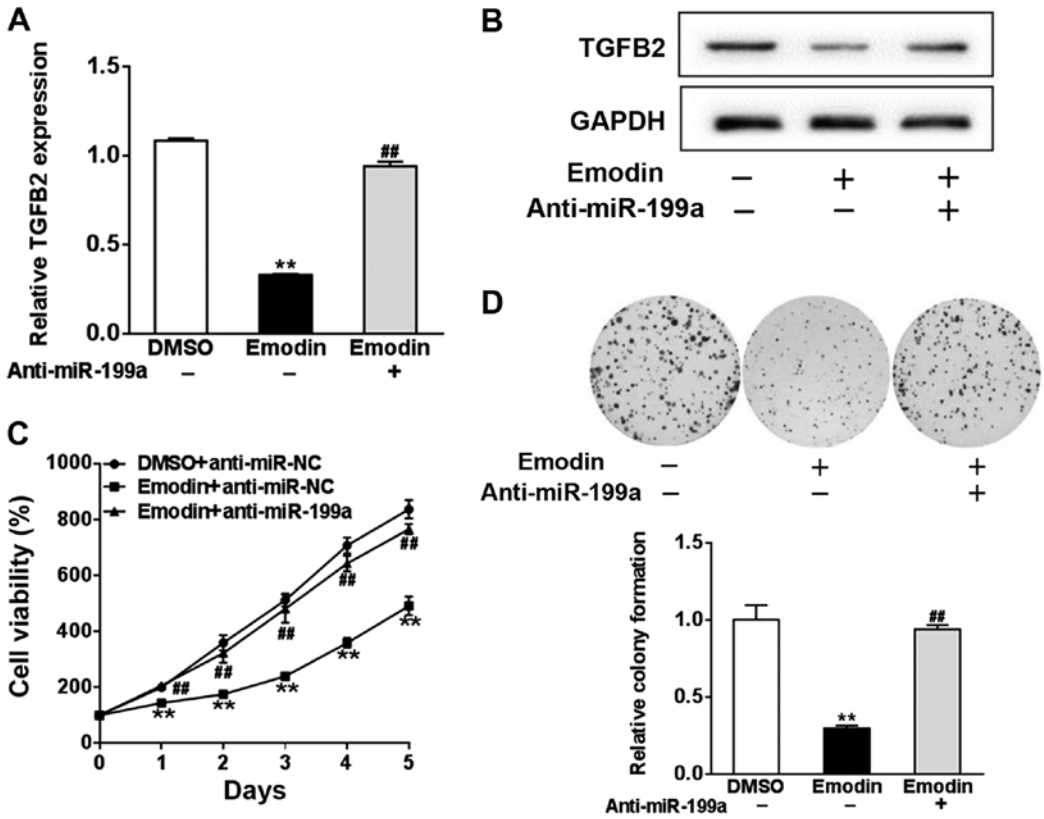

Figure 4. Silencing of miR-199a restores the suppression of TGF-β2 induced by emodin in ovarian cancer cells. (A and B) A2780 cells were transfected with miR-199a inhibitor (anti-miR-199a), or control antisense RNA (anti-miR-NC). After overnight incubation, the cells were treated with 20 μM emodin or DMSO. After 48 h, the expression levels of TGF-β2 were assessed by qRT-PCR and western blotting. (C) Cells were seeded in a 96-well plate and transfected with anti-miR-199a, or control anti-miR-NC. Emodin (20 μM) was added into each well after an overnight incubation. After 48 h of transfection, CCK-8 assay was used to detected cell viability. (D) Colony formation efficiency was measured by counting the number of colonies growing in soft agar. All data are presented as the means ± SD from three independent experiments with triple replicates per experiment. **P<0.01 indicates a significant difference compared to the anti-miR-NC + DMSO group. $^{\#\#}$P<0.01 indicates a significant difference compared to anti-miR-NC + emodin group.

that noted in the untreated cells from 6 h, and further reductions were observed after 12 and 24 h (P<0.01, Fig. 1B).

Elevated expression of miR-199a is induced by emodin. We identified 12 potential miRNAs that may bind to TGF-β2 using TargetScan 6.0. The expression levels of the 12 miRNAs were measured in A2780 cells treated with 20 μM emodin or DMSO for 24 h. miR-199a demonstrated a significantly higher expression level compared to miR-141, miR-200a, miR-193, miR-148a, miR-152, miR-21, miR-130, miR-301, miR-216, miR-454 and miR-590 (Fig. 2A). Then, we assessed the miR-199a expression level in A2780 cells treated with emodin for 0, 6, 12 and 24 h. A significant increase in the miR-199a level was observed from 6 h of emodin treatment (P<0.01, Fig. 2B).

miR-199a directly targets the TGF-β signaling pathway. To confirm whether miR-199a directly binds to TGF-β2, we mutated three nucleotides within the predicted miR-199a binding site of TGF-β2 3'-UTR (Fig. 3A) and performed a luciferase assay. No change in luciferase activity was observed in the cells transfected with mutated TGF-β2 compared with the negative control (miR-NC) whereas miR-199a wild-type significantly reduced the TGF-β2 transcriptional activity compared to miR-NC (P<0.01, Fig. 3B). The mRNA and protein levels of TGF-β2 were compared between A2780 cells transfected with miR-199a and cells with control miR-NC. Both transcriptional and translational levels of TGF-β2 were significantly inhibited by miR-199a (P<0.01, Fig. 3C and D). Spearman's correlation analysis revealed a significant inverse correlation between the expression of miR-199a and TGF-β2 in human ovarian cancer specimens (n=37, P<0.05, Fig. 3E).

miR-199a mediates emodin-induced TGF-β2 downregulation. To investigate whether miR-199a was affected by emodin to regulate TGF-β2, we transfected A2780 cells with miR-199a inhibitor (anti-miR-199a) or control antisense RNA (anti-miR-NC), and treated the cells with 20 μM emodin or DMSO. Protein and mRNA expression of TGF-β2 were significantly reduced by emodin treatment in comparison with DMSO, whereas anti-miR-199a inhibited the effect of emodin on TGF-β2 (P<0.01, Fig. 4A and B). Given the role of TGF-β in cell proliferation, we next assessed whether miR-199a mediated the effect of TGF-β2 on cell viability. In comparison with the untreated cells, emodin treatment significantly reduced the growth of A2780 cells, which was blocked by anti-miR-199a (P<0.01, Fig. 4C). Colony formation assay revealed that A2780 cells transfected with anti-miR-199a significantly reversed the reduction in colony formation induced by emodin (P<0.01, Fig. 4D).

Emodin inhibits TGF-β2 through the FOXD3/miR-199a signaling axis. Both primary mature miR-199a-1 and

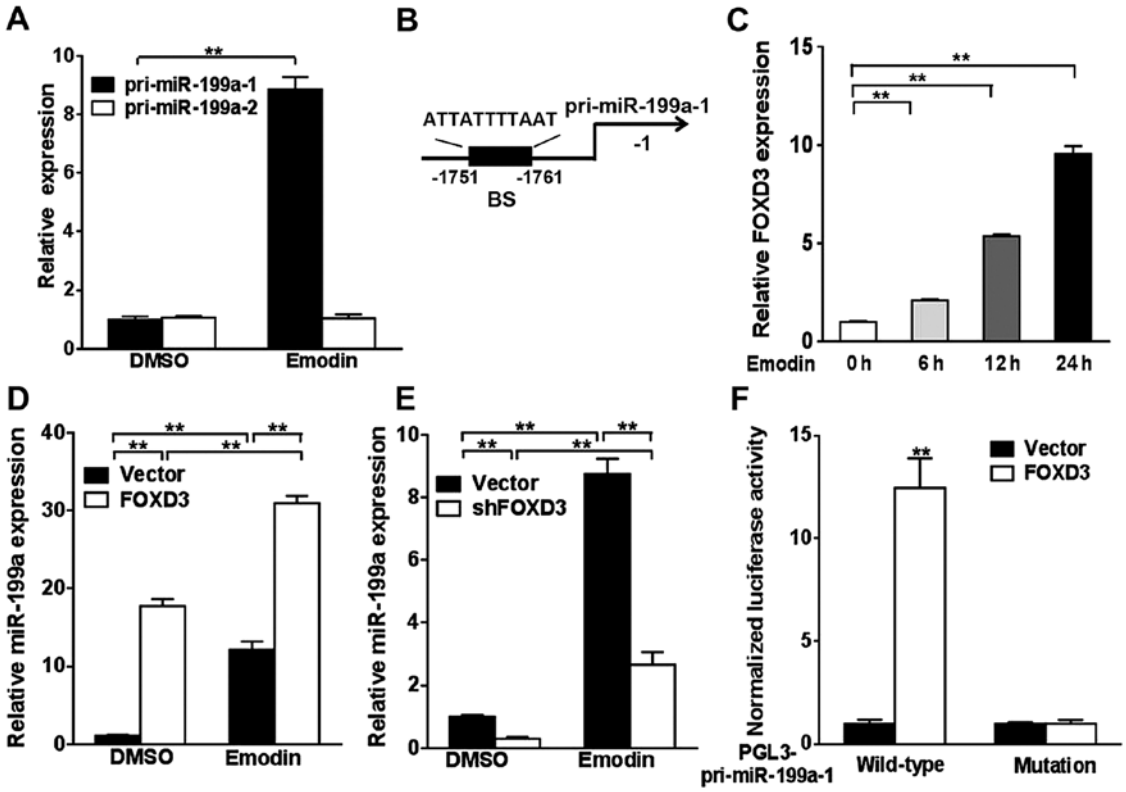

Figure 5. Upregulation of miR-199a induced by emodin is mediated through FOXD3. (A) A2780 cells were treated with 20 μM emodin or DMSO for 24 h. Relative expression levels of pri-miR-199a-1 and pri-miR-199a-2 were assessed by qRT-PCR. (B) Schematic diagram shows the potential FOXD3 binding site (BS) of miR-199a-1. (C) A2780 cells were treated with 20 μM emodin or DMSO for 0, 6, 12 or 24 h, and the FOXD3 expression levels were assessed by qRT-PCR. (D) A2780 cells were transfected with FOXD3 or control vector, and were treated with 20 μM emodin or DMSO. After 48 h, the miR-199a expression level was analyzed by qRT-PCR. (E) A2780 cells were transfected with shFOXD3 or control vector, and were treated with 20 μM emodin or DMSO. After 48 h, the miR-199a expression level was analyzed by qRT-PCR. (F) Luciferase reporter assay was performed to detect the relative luciferase activities of wild-type (WT) and mutated PGL3-miR-199a-1 reporters. Data are presented as mean ± SD from three independent experiments with triple replicates per experiment. **P<0.01.

miR-199a-2 are precursors of mature miR-199a. We analyzed their transcripts in A2780 cells treated with 20 μM emodin or DMSO for 24 h, and only pri-miR-199a-1 was regulated by emodin (Fig. 5A). Additionally, we revealed that there is a potential FOXD3 binding site within miR-199a-1 (Fig. 5B). FOXD3 is an important factor in the suppression of tumorigenesis. Emodin treatment of A2780 cells significantly increased the mRNA level of FOXD3 compared to that noted in the untreated cells (P<0.01, Fig. 5C). FOXD3 markedly promoted the expression level of miR-199a compared with the control, while emodin further enhanced this promotion (P<0.01, Fig. 5D). As expected, targeted knockdown of FOXD3 led to a significant decrease in the emodin-induced increase of miR-199a expression (P<0.01, Fig. 5E). Consistent with these results, luciferase activity of miR-199a-1 was significantly upregulated by FOXD3 compared with of a mutated miR-199a-1 reporter (mut PGL3-miR-199a-1, P<0.01, Fig. 5F).

Discussion

TGF-β functions as an inhibitor of normal cell proliferation, but the role of TGF-β in cancer progression has been widely suggested. It is an important growth factor involved in the regulation of the proliferation of ovarian surface epithelial cells where 80% of ovarian cancers originate (12) and in the promotion of ovarian cancer cell proliferation by elevating the expression level of insulin growth factor 1 receptor (13). TGF-β enhances the secretion of matrix metalloproteinases that participate in gynecological cancer metastasis (14,15). TGF-β contains three isoforms, TGF-β1, TGF-β2 and TGF-β3. An early clinical study reported that 44, 66 and 66% of malignant ovarian cancer patients demonstrated overexpression of TGF-β1, TGF-β2 and TGF-β3, respectively (16). The dual or triple co-expression of TGF-β isoforms suggests a similar role for them in ovarian cancer (16). The poor prognosis of patients with ovarian cancer was reported to be associated with TGF-β activation (17) suggesting the potential functions of TGF-β in ovarian cancer development. Our results demonstrated a reduction in TGF-β2 induced by emodin, providing supportive evidence of the antitumor property of emodin *in vitro*.

In recent years, studies have begun to concentrate on the correlation between miRNAs and cancer. miRNAs are ~22-nt RNAs that bind to the 3'-UTR of target mRNAs to negatively regulate the expression of target genes (18). Thus, overexpression of miRNAs may function as either oncogenes or tumor-suppressing genes (19). By comparing the expression profiles of miRNAs between ovarian cancer tissues and normal ovaries, Iorio *et al* (20) first discovered that several miRNAs, including miR-141, miR-200a, miR-200b and miR-200c, were

upregulated, while miR-125b1, miR-140, miR-145 and miR-199a were downregulated in ovarian cancer. As an important factor in tumorigenesis, TGF-β signaling has also been shown to be linked to several miRNAs. miR-181a was identified to promote TGF-β-induced EMT by inhibiting Smad7, a negative regulator of TGF-β (17). Additionally, miR-200 was reported to inhibit TGF-β signaling to suppress cell invasion and upregulate epithelial gene expression (21). The present study demonstrated that TGF-β2 expression was significantly reduced in A2780 cells treated with emodin. To identify whether miRNAs have a role in regulating TGF-β2, we used TargetScan to predict the miRNAs with conserved binding sites to TGF-β2, and found that miR-199a was a potential regulator of TGF-β2. This was further evidenced by the influence of emodin at both the transcriptional and translational levels of TGF-β2. Thus, regarding the low expression level of miR-199a in ovarian cancer shown in previous studies, it is possible that emodin exerts it functions via upregulating miR-199a to repress TGF-β2 signaling in ovarian cancer cell lines *in vitro*.

To date, few miRNAs have been identified to be modulated by emodin including angiogenesis-associated miR-155, miR-210 and miR-20b (4). The combination of emodin and curcumin synergistically increased miR-34a expression conferring an antitumor effect against breast cancer (22). However, there are several miRNAs reported in previous studies that are involved in controlling the TGF-β2 signaling pathway. miR-153 was demonstrated to inhibit proliferation and invasion of osteosarcoma cells by repressing TGF-β2 (23). Evidence showed that TGF-β2 also plays a crucial role in glioma cell proliferation and metastasis, which can be repressed by miR-141 (24). miR-200a at a high level in ovarian cancer cells was found to directly target TGF-β2 to inhibit renal carcinoma cell proliferation, migration and invasion (25). We also observed statistical significance in the correlation between miR-200a and TGF-β2, but miR-191a showed a much higher significant relevance to TGF-β2. This may be caused by the distinction between different types of tumors. Furthermore, we revealed that miR-199a was involved in emodin-induced antitumor effect *in vitro*, and both transcriptional and translational levels of TGF-β2 were increased by miR-199a. In particular, only pri-miR-199a-1 was influenced by emodin. A potential binding sites of FOXD3 was found within miR-199a.

We observed that the alteration of miR-199a induced by emodin was mediated by FOXD3, known as an important factor in the development of chemoresistance via enhancing EMT (26). Previous studies have demonstrated the involvement of FOXD3 in tumorigenesis in several types of cancers, such as human hepatocellular carcinoma (27) colorectal cancer (28) and gastric carcinogenesis (29). No studies have characterized the function of FOXD3 in ovarian cancer, but its role in the regulation of miR-137 has been studied. FOXD3 directly controls the transcriptional activity of miR-137 to suppress the growth and metastasis of hepatocellular carcinoma (27). Of note, miR-137 expression was reported to be reduced in ovarian cancer specimens, and its function as a tumor suppressor was evidenced (30) suggesting that FOXD3 may be also be dysregulated in ovarian cancer. This needs to be evidenced in further study. Our results indicated that FOXD3 expression was significantly increased by emodin treatment in ovarian cancer cells *in vitro*. Thus, it is possible that emodin directly enhanced FOXD3 expression and sequentially activated miR-199a, which inhibited the expression of TGF-β2 in ovarian cancer cells *in vitro*.

Together, the present study demonstrated a possible signaling pathway activated by emodin in a cisplatin-resistant ovarian cancer cell line. We identified that emodin exerts antitumor effect via activating FOXD3 and miR-199a to suppress the TGF-β2 expression which is at high level in ovarian cancer tumors. Nevertheless, experiments performed in the present study were exclusively *in vitro*, which limited the further clinical significance of our results. Further studies are needed to expand our understanding of the antitumor function of emodin, in order to potentiate its clinical applications.

Acknowledgements

Not applicable.

Funding

No funding was received.

Availability of data and materials

All data generated or analyzed during this study are included in this published article.

Authors' contributions

SKJ and LT carried out the research, data acquisition and drafted the manuscript, CYL and DYC provided assistance for data acquisition, data analysis and statistical analysis, WYK and YQ designed the research, manuscript editing and manuscript review. SKJ and LT Contributed equally. All authors have read and approved the content of the manuscript.

Ethics approval and consent to participate

Not applicable.

Consent for publication

Not applicable.

Competing interests

The authors declare that they have no competing interests.

References

1. Siegel RL, Miller KD and Jemal A: Cancer statistics, 2016. CA Cancer J Clin 66: 7-30, 2016.
2. Chen W, Zheng R, Baade PD, Zhang S, Zeng H, Bray F, Jemal A, Yu XQ and He J: Cancer statistics in China, 2015. CA Cancer J Clin 66: 115-132, 2016.
3. Dong X, Fu J, Yin X, Cao S, Li X, Lin L and Ni J; Huyiligeqi: Emodin: A review of its pharmacology, toxicity and pharmacokinetics. Phytother Res 30: 1207-1218, 2016.
4. Lin SZ, Xu JB, Ji X, Chen H, Xu HT, Hu P, Chen L, Guo JQ, Chen MY, Lu D, *et al*: Emodin inhibits angiogenesis in pancreatic cancer by regulating the transforming growth factor-β/drosophila mothers against decapentaplegic pathway and angiogenesis-associated microRNAs. Mol Med Rep 12: 5865-5871, 2015.

5. Guo J, Xiao B, Liu Q, Gong Z and Le Y: Suppression of C-myc expression associates with anti-proliferation of aloe-emodin on gastric cancer cells. Cancer Invest 26: 369-374, 2008.
6. Suboj P, Babykutty S, Srinivas P and Gopala S: Aloe emodin induces G2/M cell cycle arrest and apoptosis via activation of caspase-6 in human colon cancer cells. Pharmacology 89: 91-98, 2012.
7. Xie MJ, Ma YH, Miao L, Wang Y, Wang HZ, Xing YY, Xi T and Lu YY: Emodin-provoked oxidative stress induces apoptosis in human colon cancer HCT116 cells through a p53-mitochondrial apoptotic pathway. Asian Pac J Cancer Prev 15: 5201-5205, 2014.
8. Gao R, Chen R, Cao Y, Wang Y, Song K, Zhang Y and Yang J: Emodin suppresses TGF-β1-induced epithelial-mesenchymal transition in alveolar epithelial cells through Notch signaling pathway. Toxicol Appl Pharmacol 318: 1-7, 2017.
9. Hsu HC, Liu LC, Wang HY, Hung CM, Lin YC, Ho CT and Way TD: Stromal fibroblasts from the interface zone of triple negative breast carcinomas induced epithelial-mesenchymal transition and its inhibition by emodin. PLoS One 12: e0164661, 2017.
10. Li J, Liu P, Mao H, Wanga A and Zhang X: Emodin sensitizes paclitaxel-resistant human ovarian cancer cells to paclitaxel-induced apoptosis *in vitro*. Oncol Rep 21: 1605-1610, 2009.
11. Ma J, Yang J, Wang C, Zhang N, Dong Y, Wang C, Wang Y and Lin X: Emodin augments cisplatin cytotoxicity in platinum-resistant ovarian cancer cells via ROS-dependent MRP1 downregulation. BioMed Res Int 2014: 107671, 2014.
12. Auersperg N, Wong AS, Choi KC, Kang SK and Leung PC: Ovarian surface epithelium: Biology, endocrinology, and pathology. Endocr Rev 22: 255-288, 2001.
13. Alsina-Sanchis E, Figueras A, Lahiguera Á, Vidal A, Casanovas O, Graupera M, Villanueva A and Viñals F: The TGFβ pathway stimulates ovarian cancer cell proliferation by increasing IGF1R levels. Int J Cancer 139: 1894-1903, 2016.
14. Lin SW, Lee MT, Ke FC, Lee PP, Huang CJ, Ip MM, Chen L and Hwang JJ: TGFbeta1 stimulates the secretion of matrix metalloproteinase 2 (MMP2) and the invasive behavior in human ovarian cancer cells, which is suppressed by MMP inhibitor BB3103. Clin Exp Metastasis 18: 493-499, 2000.
15. Peng H, Liu L and Zhao X: Prognostic significance of matrix metalloproteinase-2 in gynecological cancer: A systemic review of the literature and meta-analysis. J BUON 18: 202-210, 2013.
16. Bartlett JM, Langdon SP, Scott WN, Love SB, Miller EP, Katsaros D, Smyth JF and Miller WR: Transforming growth factor-beta isoform expression in human ovarian tumours. Eur J Cancer 33: 2397-2403, 1997.
17. Parikh A, Lee C, Joseph P, Marchini S, Baccarini A, Kolev V, Romualdi C, Fruscio R, Shah H, Wang F, *et al*: microRNA-181a has a critical role in ovarian cancer progression through the regulation of the epithelial-mesenchymal transition. Nat Commun 5: 2977, 2014.
18. Moss EG: MicroRNAs: Hidden in the genome. Curr Biol 12: R138-R140, 2002.
19. Lewis BP, Shih IH, Jones-Rhoades MW, Bartel DP and Burge CB: Prediction of mammalian microRNA targets. Cell 115: 787-798, 2003.
20. Iorio MV, Visone R, Di Leva G, Donati V, Petrocca F, Casalini P, Taccioli C, Volinia S, Liu CG, Alder H, *et al*: MicroRNA signatures in human ovarian cancer. Cancer Res 67: 8699-8707, 2007.
21. Perdigão-Henriques R, Petrocca F, Altschuler G, Thomas MP, Le MT, Tan SM, Hide W and Lieberman J: miR-200 promotes the mesenchymal to epithelial transition by suppressing multiple members of the Zeb2 and Snail1 transcriptional repressor complexes. Oncogene 35: 158-172, 2016.
22. Guo J, Li W, Shi H, Xie X, Li L, Tang H, Wu M, Kong Y, Yang L, Gao J, *et al*: Synergistic effects of curcumin with emodin against the proliferation and invasion of breast cancer cells through upregulation of miR-34a. Mol Cell Biochem 382: 103-111, 2013.
23. Niu G, Li B, Sun L and An C: MicroRNA-153 inhibits osteosarcoma cells proliferation and invasion by targeting TGF-β2. PLoS One 10: e0119225, 2015.
24. Peng T, Zhang S, Li W, Fu S, Luan Y and Zuo L: MicroRNA-141 inhibits glioma cells growth and metastasis by targeting TGF-β2. Am J Transl Res 8: 3513-3521, 2016.
25. Lu R, Ji Z, Li X, Qin J, Cui G, Chen J, Zhai Q, Zhao C, Zhang W and Yu Z: Tumor suppressive microRNA-200a inhibits renal cell carcinoma development by directly targeting TGFB2. Tumour Biol 36: 6691-6700, 2015.
26. Zhou Z, Zhang L, Xie B, Wang X, Yang X, Ding N, Zhang J, Liu Q, Tan G, Feng D, *et al*: FOXC2 promotes chemoresistance in nasopharyngeal carcinomas via induction of epithelial mesenchymal transition. Cancer Lett 363: 137-145, 2015.
27. Liu LL, Lu SX, Li M, Li LZ, Fu J, Hu W, Yang YZ, Luo RZ, Zhang CZ and Yun JP: FoxD3-regulated microRNA-137 suppresses tumour growth and metastasis in human hepatocellular carcinoma by targeting AKT2. Oncotarget 5: 5113-5124, 2014.
28. He GY, Hu JL, Zhou L, Zhu XH, Xin SN, Zhang D, Lu GF, Liao WT, Ding YQ and Liang L: The FOXD3/miR-214/MED19 axis suppresses tumour growth and metastasis in human colorectal cancer. Br J Cancer 115: 1367-1378, 2016.
29. Cheng AS, Li MS, Kang W, Cheng VY, Chou JL, Lau SS, Go MY, Lee CC, Ling TK, Ng EK, *et al*: *Helicobacter pylori* causes epigenetic dysregulation of *FOXD3* to promote gastric carcinogenesis. Gastroenterology 144: 122-133.e9, 2013.
30. Zhang L, Li Z, Gai F and Wang Y: MicroRNA-137 suppresses tumor growth in epithelial ovarian cancer *in vitro* and *in vivo*. Mol Med Rep 12: 3107-3114, 2015.